A Reliable Method of Preparation of Diiridium Paddlewheel Complexes: Structures of the First Compounds with Ir_2^{5+} Cores

F. Albert Cotton,*,† Chun Lin,† and Carlos A. Murillo*,†,‡

Department of Chemistry and Laboratory for Molecular Structure and Bonding, Texas A&M University, P.O. Box 30012, College Station, Texas 77842-3012, and Department of Chemistry, University of Costa Rica, Ciudad Universitaria, Costa Rica

Received May 18, 2000

Paddlewheel complexes with Ir_2^{5+} cores and having an unpaired electron have been made for the first time. These have been prepared by reacting $(COD)Ir^{I}(DArF)_2Ir^{III}(CF_3CO_2)_2(H_2O)$ with two molar equivalents of HDArF (DArF = *N,N′*-diarylformamidinate, Ar = *p*-anisyl and *p*-chlorophenyl, and COD = 1,5-cyclooctadiene). In the presence of CH_2Cl_2, the corresponding $Ir_2(\mu\text{-DArF})_4(\eta^1\text{-O}_2CCF_3)\cdot 2CH_2Cl_2$ compounds are isolated in ca. 50% yield. The metal−metal distances are 2.5073(9) and 2.513(1) Å for the *p*-anisyl and *p*-chlorophenyl derivatives, respectively. We also report the structure of the dinuclear compound $[Ir_2(cis\text{-}\mu\text{-DAniF})_2(MeCN)_6](BF_4)_2\cdot 2CH_3CN$, which has an Ir−Ir bond distance of 2.6019(4) Å, and that of a starting material, $[Ir(DAniF)(COD)]_2\cdot$toluene.

Introduction

Dinuclear paddlewheel-type complexes with elements of the third transition series from tungsten to platinum are relatively well-known,[1] an exception being iridium. These complexes typically have two metal atoms linked by four bridging ligands; some also have axial ligands. Depending on the electronic configuration of the metal atoms and the type of ligands, metal-to-metal bond orders can vary from 0.5 (e.g., $Pt_2(DTolF)_4^{+}$)[2,3] to 4 (e.g., $Re_2(DTolF)_4Cl_2$).[4]

For iridium, there are several compounds with Ir_2^{4+} cores having M−M single bonds,[1] but only one of them is of the paddlewheel type, namely, $Ir_2(DTolF)_4$.[5] However, the poor yield reported for the latter discouraged further studies of this or other diiridium paddlewheel complexes. More recently we made the first complex, also of the paddlewheel type, with a double-bonded Ir_2^{6+} core,[6] $Ir_2(hpp)_4Cl_2$ (where hpp is the anion of 1,3,4,6,7,8-hexahydro-*2H*-pyrimido[1,2-*a*]pyrimidine), but again yields were quite low (approximately 10%).

In our continuing search for better preparative methods, we have returned to the route originally developed by Cotton and Poli,[5] and, as explained herein, found that it is possible to improve and extend it.

Experimental Section

General Considerations. All the syntheses were performed under a dry nitrogen atmosphere using standard Schlenk techniques. Solvents were dried and then distilled under nitrogen following conventional methods. All starting materials were purchased from Aldrich and used as received. The ligands HDAniF and $HDPh^{Cl}F$[7] and complexes $[IrCl(COD)]_2$ (COD = 1,5-cycoloctadiene),[8] $[Ir(DAniF)(COD)]_2$,[9] $[Ir(DPh^{Cl}F)(COD)]_2$,[9] $Ir_2(DAniF)_2(O_2CCF_3)_2(COD)(H_2O)$,[10] $Ir_2(DPh^{Cl}F)_2(O_2CCF_3)_2(COD)(H_2O)$,[10] and $[Ir_2(DAniF)_2(CH_3CN)_6](BF_4)_2$[11] were prepared following essentially the same procedures as those published for the corresponding di-*p*-tolylformamidinate analogues; their purity was confirmed by ^{1}H NMR.[12] Elemental analyses were performed by the Canadian Microanalytical Service, Delta, British Columbia. X-band EPR spectra in frozen dichloromethane were recorded on a Bruker model ESP 300 spectrometer equipped with an Oxford Instruments ESR 900 cryostat (100 K). ^{1}H NMR spectra were recorded on an XL-200E NMR spectrometer, with chemical shifts (δ) referenced to the corresponding solvent.

Preparation of $Ir_2(\mu\text{-DArF})_4(\eta^1\text{-O}_2CCF_3)\cdot 2CH_2Cl_2$ Complexes. The following procedure was used for preparation of the anisyl compound. A mixture of $Ir_2(DAniF)_2(O_2CCF_3)_2(COD)(H_2O)$ (375 mg, 0.300 mmol) and the neutral formamidine HDAniF (154 mg, 0.600 mmol) in 40 mL of toluene was warmed to 90 °C for 6 h under stirring, during which time the color of the solution gradually changed from dark green to a lighter shade of green. The solvent was removed from the resulting mixture under vacuum. The residue was then extracted with 10 mL of CH_2Cl_2, and layering of the CH_2Cl_2 solution with hexanes provided large dark green crystals of $Ir_2(\mu\text{-DAniF})_4(\eta^1\text{-O}_2\text{-}$

---

† Texas A&M University.

‡ University of Costa Rica.

[1] Cotton, F. A.; Walton, R. A. *Multiple Bonds between Metal Atoms*; Oxford University Press: Oxford, 1993.

[2] Throughout this paper the formamidinate anions $ArNC(H)NAr^-$ will be abbreviated as $DAniF^-$, $DTolF^-$ and $DPh^{Cl}F^-$, for the Ar groups *p*-anisyl, *p*-tolyl, and *p*-chlorophenyl, respectively.

[3] Cotton, F. A.; Matonic, J. H.; Murillo, C. A. *Inorg. Chim. Acta* **1997**, *264*, 61−64.

[4] Cotton, F. A.; Ren, T. *J. Am. Chem. Soc.* **1992**, *114*, 2495−2502.

[5] Cotton, F. A.; Poli, R. *Polyhedron* **1987**, *6*, 1625−1628.

[6] Cotton, F. A.; Murillo, C. A.; Timmons, D. J. *Chem. Commun.* **1999**, 1427−1428.

[7] Lin, C.; Protasiewicz, J. D.; Smith, E. T.; Ren, T. *Inorg. Chem.* **1996**, *35*, 6422−6428.

[8] Herde, J. L.; Lambert, J. C.; Senoff, C. V. *Inorg. Synth.* **1974**, *15*, 18−19.

[9] Cotton, F. A.; Poli, R. *Inorg. Chim. Acta* **1986**, *122*, 243−248.

[10] Cotton, F. A.; Poli, R. *Inorg. Chem.* **1987**, *26*, 590−595.

[11] Dunbar, K. R.; Majors, S. O.; Sun J.-S. *Inorg. Chim. Acta* **1995**, *229*, 373−382.

[12] ^{1}H NMR data: $[Ir(DAniF)(COD)]_2$, δ (ppm, in C_6D_6) 7.91 (s, 2H), 7.54−6.80 (m, 16H), 4.16 (br, 4H), 3.86 (br, 4H), 3.34 (s, 12H), 2.87 (br, 4H), 2.42 (br, 4H), 1.77 (br, 4H), 1.61 (br, 4H). $[Ir(DPh^{Cl}F)(COD)]_2$, δ (ppm, in C_6D_6) 7.45 (s, 2H), 7.20−7.05 (m, 16H), 3.89 (br, 4H), 3.58 (br, 4H), 2.67 (br, 4H), 2.21 (br, 4H), 1.61 (d, 4H), 1.46 (d, 4H). $Ir_2(DAniF)_2(O_2CCF_3)_2(COD)(H_2O)$, δ (ppm, in C_6D_6) 9.43 (s, 2H), 7.48 (s, 2H), 7.20−6.67 (m, 16H), 5.38 (br, 2H), 4.05 (br, 2H), 3.28 (s, 6H), 3.26 (s, 6H), 3.03 (br, 2H), 2.00−1.68 (m, 6H). $Ir_2(DPh^{Cl}F)_2(O_2CCF_3)_2(COD)(H_2O)$, δ (ppm, in C_6D_6) 9.28 (s, 2H), 7.12 (d, 4H), 7.01 (s, 2H), 6.99 (d, 4H), 6.81 (d, 4H), 6.45 (d, 4H), 5.09 (br, 2H), 3.78 (br, 2H), 2.83 (br, 2H), 1.75−1.30 (m, 6H). $[Ir_2(DAniF)_2(CH_3CN)_6](BF_4)_2$, δ (ppm, in CD_3CN) 7.65 (s, 2H), 6.94 (d, 8H), 6.81 (d, 8H), 3.79 (s, 12H).

10.1021/ic000527c CCC: $19.00

Table 1. Crystal and Structure Refinement Data

	$Ir_2(\mu\text{-DAniF})_4(\eta^1\text{-}O_2CCF_3)\cdot 2CH_2Cl_2$	$Ir_2(\mu\text{-DPh}^{Cl}F)_4(\eta^1\text{-}O_2CCF_3)\cdot 2CH_2Cl_2$	$[Ir(DAniF)(COD)]_2\cdot$ toluene	$[Ir_2(cis\text{-}\mu\text{-DAniF})_2(CH_3CN)_6](BF_4)_2\cdot 2CH_3CN$
empirical formula	$C_{64}H_{64}Cl_4F_3Ir_2N_8O_{10}$	$C_{55}H_{38}Cl_{10}F_3Ir_2N_8O_2$	$C_{53}H_{62}Ir_2N_4O_4$	$C_{44}H_{51}B_2F_8Ir_2N_{11}O_4$
fw	1688.43	1638.83	1203.47	1355.98
space group	*Pbcn*	*P*2/*n*	*P*2$_1$/*c*	*P*2/*n*
a, Å	23.225(2)	14.107(4)	9.195(3)	12.9795(3)
b, Å	24.799(7)	12.510(2)	27.420(3)	16.3959(5)
c, Å	22.912(3)	16.406(3)	18.306(5)	13.831(1)
β, deg		90.51(2)	90.16(2)	116.987(4)
vol, Å^3	13196(4)	2895(1)	4615(2)	2622.9(2)
Z	8	2	4	2
T, °C	173(2)	213(2)	173(2)	213(2)
λ, Å	0.710 73	0.710 73	0.710 73	0.710 73
ρ_{calcd}, g cm^{-3}	1.700	1.880	1.732	1.717
μ, mm^{-1}	4.263	5.113	5.812	5.148
R1,[a] wR2[b]	0.043, 0.092	0.063, 0.136	0.030, 0.072	0.028, 0.068
R1, wR2	0.133, 0.116	0.082, 0.160	0.051, 0.077	0.031, 0.070

[a] $R1 = [\Sigma w(F_o - F_c)^2/\Sigma wF_o^2]^{1/2}$. [b] $wR2 = [\Sigma[w(F_o^2 - F_c^2)^2]/\Sigma w(F_o2)^2]^{1/2}$, $w = 1/[\sigma^2(F_o^2) + (aP)^2 + bP]$, where $P = [\max(F_o^2 \text{ or } 0) + 2(F_c^2)]/3$.

$CCF_3)\cdot 2CH_2Cl_2$ after several days; yield 268 mg (53%). The crystals were then dried under vacuum for elemental analysis. Anal. for $Ir_2(DAniF)_4(O_2CCF_3)$, $C_{62}H_{60}F_3N_8O_{10}Ir_2$, Calcd (Found): C, 49.04 (49.15), H, 3.98 (4.11), N, 7.38 (7.40). A similar method was used to prepare $Ir_2(\mu\text{-DPh}^{Cl}F)_4(\eta^1\text{-}O_2CCF_3)\cdot 2CH_2Cl_2$ in 56% yield. Anal. for $Ir_2(\mu\text{-DPh}^{Cl}F)_4(\eta^1\text{-}O_2CCF_3)$, $C_{54}H_{36}Cl_8F_3N_8O_2Ir_2$, Calcd (Found): C, 41.74 (42.03), H, 2.34 (2.45), N, 7.21 (7.12).

X-ray Crystallographic Procedures. Single-crystal X-ray work on $Ir_2(\mu\text{-DPh}^{Cl}F)_4(\eta^1\text{-}O_2CCF_3)\cdot 2CH_2Cl_2$ and $Ir_2(cis\text{-}\mu\text{-DAniF})_2(CH_3CN)_6(BF_4)_2\cdot 2CH_3CN$ was performed on a Nonius FAST diffractometer at −60 °C utilizing the program MADNES.[13] In each case a suitable crystal was mounted on the tip of a quartz fiber with a small amount of silicone grease and transferred to a goniometer head. Cell parameters were obtained from an auto-indexing routine by refining 250 reflections within a 2θ range of 18.1−41.6°. Cell dimensions and Laue symmetry for all crystals were confirmed with axial photographs. All data were corrected for Lorentz and polarization effects. Data were processed using an ellipsoid-mask algorithm (program PROCOR[14]), and the program SORTAV[15] was used to correct for absorption.

Single-crystal X-ray data for $[Ir(DAniF)(COD)]_2\cdot$toluene and $Ir_2(\mu\text{-DAniF})_4(\eta^1\text{-}O_2CCF_3)\cdot 2CH_2Cl_2$ were collected on a Nonius CAD4 diffractometer at −100 °C. Unit cell refinement utilized 25 strong reflections in the range of $28.1° \leq 2\theta \leq 33.1°$ for $[Ir(DAniF)(COD)]_2\cdot$toluene and $28.1° \leq 2\theta \leq 33.0°$ for $Ir_2(\mu\text{-DAniF})_4(\eta^1\text{-}O_2CCF_3)\cdot 2CH_2Cl_2$. Empirical absorption corrections based on ψ-scans were applied. Data were processed into SHELX format using the program XCAD. All other data collection procedures were similar to those used on the FAST diffractometer (vide supra).

In all structures, the positions of some or all of the non-hydrogen atoms were found via direct methods by way of the program package SHELXTL.[16] For all structures, subsequent cycles of least-squares refinement followed by difference Fourier syntheses revealed the positions of the remaining non-hydrogen atoms. All hydrogen atoms were placed in calculated positions. As shown in Figure 1, the molecule of $Ir_2(\mu\text{-DPh}^{Cl}F)_4(\eta^1\text{-}O_2CCF_3)\cdot 2CH_2Cl_2$ exhibits a disorder along the 2-fold axis. The molecule was successfully refined as a pair, comprising a major orientation and a minor orientation, with a ratio of 0.52:0.48. Other details of data collection and refinement for all complexes are given in Table 1. Selected atomic distances and angles are provided in Table 2. Other crystallographic data are available as Supporting Information.

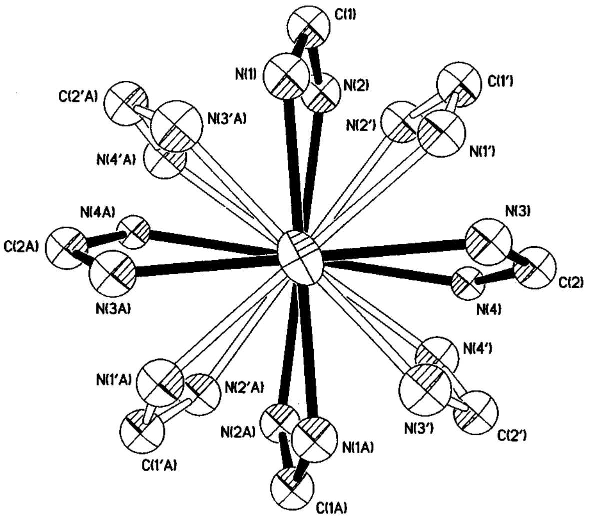

Figure 1. A view of the core of the $Ir_2(\mu\text{-DPh}^{Cl}F)_4(\eta^1\text{-}O_2CCF_3)\cdot 2CH_2Cl_2$ molecule, showing the nature of the disorder. The occupancy of the major orientation (solid bonds) is 52%.

Results and Discussion

Synthetic Considerations. The present synthetic work builds upon the route previously established to make $Ir_2(DTolF)_4$ in low yield,[5] as shown in Scheme 1. The preparation of $(COD)Ir(\mu\text{-}Cl)_2Ir(COD)$ has long been known.[8] The next reaction, with HDArF to give $(COD)Ir(\mu\text{-DArF})_2Ir(COD)$, followed by the reaction of this with $Ag(CF_3CO_2)$ to give $(COD)Ir^I(\mu\text{-DArF})_2Ir^{III}(CF_3CO_2)_2(H_2O)$ was first described by Cotton and Poli[9,10] for the case where Ar = *p*-tolyl. From this point on, three different paths may be followed.

Cotton and Poli[5] showed that the mixed-valent intermediate would react in toluene to give $Ir_2(DTolF)_4$. More recently Dunbar et al.[11] showed that when the mixed valence species is treated with $(Et_3O)BF_4$ in acetonitrile, the compound $[Ir_2(cis\text{-}\mu\text{-DTolF})_2(CH_3CN)_6][BF_4]_2$ is obtained.

In this work we have first shown that the DAniF analogues of the $(COD)Ir(\mu\text{-DTolF})_2Ir(COD)$ and $(COD)Ir^I(\mu\text{-DTolF})_2Ir^{III}(CF_3CO_2)_2(H_2O)$ intermediates can be made and have characterized the former crystallographically. We have also shown that the latter can be converted to $[Ir_2(cis\text{-}\mu\text{-DAniF})_2(CH_3CN)_6](BF_4)_2$, an analogue of Dunbar's compound.

However, the important new reaction that is reported here (see pathway 3 in Scheme 2) is that when the mixed-valent

---

(13) Pflugrath, J.; Messerschmitt, A. MADNES, Munich Area Detector (New EEC) System, Version EEC 11/1/89, with enhancements by Nonius Corp., Delft, The Netherlands. A description of MADNES appears in Messerschmitt, A.; Pflugrath, J. *J. Appl. Crystallogr.* **1987**, *20*, 306−315.

(14) (a) Kabsch, W. *J. Appl. Crystallogr.* **1988**, *21*, 67−71. (b) Kabsch, W. *J. Appl. Crystallogr.* **1988**, *21*, 916−924.

(15) Blessing, R. H. *Acta Crystallogr.* **1995**, *A51*, 33−38.

(16) SHELXTL, Version 5.03, Siemens Industrial Automation Inc., Madison, WI.

Table 2. Selected Bond Distances (Å) and Angles (deg)

		$Ir_2(\mu\text{-DAniF})_4(\eta^1\text{-}O_2CCF_3)\cdot 2CH_2Cl_2$			
Ir(1)−Ir(2)	2.5073(9)	Ir(2)−N(2)	2.028(10)	O(9)−(5)	1.21(2)
Ir(1)−N(3)	2.008(9)	Ir(2)−N(6)	2.050(10)	O(10)−(5)	1.30(2)
Ir(1)−N(5)	2.022(9)	Ir(2)−N(4)	2.059(9)	C(5)−(6)	1.53(2)
Ir(1)−N(1)	2.034(9)	Ir(2)−N(8)	2.060(9)		
Ir(1)−N(7)	2.046(10)	Ir(2)−O(9)	2.139(8)		
N(3)−Ir(1)−N(5)	90.8(4)	N(7)−Ir(1)−Ir(2)	87.5(2)	N(6)−Ir(2)−O(9)	93.9(3)
N(3)−Ir(1)−N(1)	88.6(4)	N(2)−Ir(2)−N(6)	172.2(4)	N(4)−Ir(2)−O(9)	98.0(3)
N(5)−Ir(1)−N(1)	173.9(4)	N(2)−Ir(2)−N(4)	91.0(4)	N(8)−Ir(2)−O(9)	90.3(3)
N(3)−Ir(1)−N(7)	174.1(4)	C(5)−O(9)−Ir(2)	137.1(8)	N(2)−Ir(2)−Ir(1)	85.9(3)
N(5)−Ir(1)−N(7)	89.4(4)	N(6)−Ir(2)−N(4)	91.3(4)	N(6)−Ir(2)−Ir(1)	86.9(3)
N(1)−Ir(1)−N(7)	90.5(4)	N(2)−Ir(2)−N(8)	89.8(4)	N(4)−Ir(2)−Ir(1)	85.9(3)
N(3)−Ir(1)−Ir(2)	86.6(3)	N(6)−Ir(2)−N(8)	86.8(4)	N(8)−Ir(2)−Ir(1)	85.8(3)
N(5)−Ir(1)−Ir(2)	86.0(3)	N(4)−Ir(2)−N(8)	171.6(4)	O(9)−Ir(2)−Ir(1)	176.0(2)
N(1)−Ir(1)−Ir(2)	87.8(3)	N(2)−Ir(2)−O(9)	93.2(3)		
		$Ir_2(\mu\text{-DPh}^{Cl}F)_4(\eta^1\text{-}O_2CCF_3)\cdot 2CH_2Cl_2$			
Ir(1)−Ir(2)	2.5130(10)	Ir(1)−N(1′)	2.02(2)	Ir(2)−N(2′)	2.07(2)
Ir(1)−N(3′)	1.95(2)	Ir(2)−N(2)	2.03(2)	Ir(2)−O(1)	2.16(2)
Ir(1)−N(1)	1.96(2)	Ir(2)−N(4)	2.04(2)		
Ir(1)−N(3)	2.00(2)	Ir(2)−N(4′)	2.05(2)		
N(3′)#1CIr(1)−N(3′)	173.6(12)	N(1′)−Ir(1)−N(1′)#1	173.8(11)	N(4′)#1CIr(2)−N(4′)	174.6(11)
N(1)−Ir(1)−N(1)#1	177.3(11)	N(3′)#1CIr(1)−Ir(2)	86.8(6)	N(2)−Ir(2)−O(1)	94.6(6)
N(1)−Ir(1)−N(3)	89.5(9)	N(1′)−Ir(1)−Ir(2)	86.9(5)	N(4)−Ir(2)−O(1)	94.3(5)
N(1)#1CIr(1)−N(3)	90.4(9)	N(2)−Ir(2)−Ir(1)	85.4(6)	N(4′)−Ir(2)−O(1)	92.7(5)
N(1)−Ir(1)−N(3)#1	90.4(9)	N(4)−Ir(2)−Ir(1)	85.7(5)	N(4′)−Ir(2)−N(2′)	90.8(9)
N(1)−Ir(1)−Ir(2)	88.6(6)	N(2)#1CIr(2)−N(2)	170.7(11)	N(2′)#1CIr(2)−N(2′)	174.0(11)
N(3)−Ir(1)−N(3)#1	177.4(11)	N(2)#1CIr(2)−N(4)	87.6(9)	N(2′)−Ir(2)−O(1)	93.0(5)
N(3′)#1CIr(1)−N(1′)	90.7(9)	N(2)−Ir(2)−N(4)	91.7(9)	N(4′)−Ir(2)−Ir(1)	87.3(5)
N(3′)−Ir(1)−N(1′)	89.0(9)	N(4′)−Ir(2)−N(2′)#1	88.9(9)	N(2′)−Ir(2)−Ir(1)	87.0(5)
N(3)−Ir(1)−Ir(2)	88.7(6)	N(2)−Ir(2)−N(4)#1	87.6(9)	O(1)−Ir(2)−Ir(1)	180.0
N(3′)−Ir(1)−N(1′)#1	90.7(9)	N(4)−Ir(2)−N(4)#1	171.4(10)		
		$[Ir(DAniF)(COD)]_2\cdot$toluene			
Ir(2)−Ir(1)	3.2327(6)	Ir(2)−(68)	2.120(7)	Ir(1)−(53)	2.117(7)
Ir(2)−N(4)	2.091(6)	Ir(2)−N(2)	2.140(5)	Ir(1)−N(3)	2.128(6)
Ir(2)−(63)	2.110(7)	Ir(1)−N(1)	2.087(6)	Ir(1)−(56)	2.132(7)
Ir(2)−(64)	2.113(7)	Ir(1)−(52)	2.112(7)		
Ir(2)−(67)	2.117(7)	Ir(1)−(57)	2.114(7)		
N(4)−Ir(2)−(63)	94.0(3)	C(63)−Ir(2)−Ir(1)	139.1(2)	C(57)−Ir(1)−N(3)	85.6(2)
N(4)−Ir(2)−(64)	92.0(3)	C(64)−Ir(2)−Ir(1)	100.6(2)	C(53)−Ir(1)−N(3)	173.5(2)
N(4)−Ir(2)−(67)	162.9(3)	C(67)−Ir(2)−Ir(1)	88.9(2)	N(1)−Ir(1)−(56)	164.2(3)
N(4)−Ir(2)−(68)	158.6(3)	C(68)−Ir(2)−Ir(1)	119.9(2)	N(3)−Ir(1)−(56)	98.1(3)
N(4)−Ir(2)−N(2)	88.3(2)	N(2)−Ir(2)−Ir(1)	73.48(14)	N(1)−Ir(1)−Ir(2)	77.27(14)
C(63)−Ir(2)−N(2)	146.9(3)	N(1)−Ir(1)−(52)	93.9(2)	C(52)−Ir(1)−Ir(2)	139.8(2)
C(64)−Ir(2)−N(2)	173.8(2)	N(1)−Ir(1)−(57)	157.1(3)	C(57)−Ir(1)−Ir(2)	120.4(2)
C(67)−Ir(2)−N(2)	96.9(3)	N(1)−Ir(1)−(53)	92.5(2)	C(53)−Ir(1)−Ir(2)	101.3(2)
C(68)−Ir(2)−N(2)	84.7(2)	N(1)−Ir(1)−N(3)	86.7(2)	N(3)−Ir(1)−Ir(2)	72.3(2)
N(4)−Ir(2)−Ir(1)	76.9(2)	C(52)−Ir(1)−N(3)	147.2(3)	C(56)−Ir(1)−Ir(2)	89.8(2)
		$[Ir_2(cis\text{-}\mu\text{-DAniF})_2(CH_3CN)_6](BF_4)_2\cdot 2CH_3CN$			
Ir(1)−Ir(1)#1	2.6019(4)	Ir(1)−N(4)	2.006(5)	Ir(1)−N(1)	2.038(4)
Ir(1)−N(3)	1.988(5)	Ir(1)−N(2)	2.037(4)	Ir(1)−N(5)	2.209(5)
N(3)−Ir(1)−N(4)	90.9(2)	N(2)−Ir(1)−N(1)	90.0(2)	N(3)−Ir(1)−Ir(1)#1	91.58(12)
N(3)−Ir(1)−N(2)	88.1(2)	N(3)−Ir(1)−N(5)	89.2(2)	N(4)−Ir(1)−Ir(1)#1	97.93(12)
N(4)−Ir(1)−N(2)	177.8(2)	N(4)−Ir(1)−N(5)	84.2(2)	N(2)−Ir(1)−Ir(1)#1	84.11(11)
N(3)−Ir(1)−N(1)	176.6(2)	N(2)−Ir(1)−N(5)	93.8(2)	N(1)−Ir(1)−Ir(1)#1	85.39(11)
N(4)−Ir(1)−N(1)	91.1(2)	N(1)−Ir(1)−N(5)	93.8(2)	N(5)−Ir(1)−Ir(1)#1	177.71(11)

intermediate reacts with two molar equivalents of HDAniF in toluene and then the mixture is put in contact with CH_2Cl_2, it is converted to $Ir_2(\mu\text{-DAniF})_4(\eta^1\text{-}O_2CCF_3)$. It has also been shown that, for Ar = *p*-ClC_6H_4, the same type of reaction occurs to give $Ir_2(\mu\text{-DPh}^{Cl}F)_4(\eta^1\text{-}O_2CCF_3)$. Both of these new compounds have been crystallographically characterized. These are the first examples of Ir_2^{5+} paddlewheel molecules.

The final reaction leading to the two $Ir_2(\mu\text{-DArF})_4(\eta^1\text{-}O_2CCF_3)$ compounds apparently results from the ability of aliphatic chlorocarbons such as CH_2Cl_2, $CHCl_3$, and CCl_4 to act as oxidizing agents.[17] Preliminary studies of the electrochemistry of these two Ir_2^{5+} compounds have shown that they undergo both oxidation and reduction reactions, which opens up much further chemistry to explore.

Structural Results. Four compounds have been characterized by single-crystal X-ray diffraction studies. Two complexes have Ir_2^{5+} cores: $Ir_2(\mu\text{-DArF})_4(\eta^1\text{-}O_2CCF_3)$ for Ar = *p*-anisyl and *p*-chlorophenyl. The others are a starting material, namely, $[Ir(DAniF)(COD)]_2$ and a complex with an Ir_2^{4+} core, $[Ir_2(cis\text{-}\mu\text{-DAniF})_2(MeCN)_6][BF_4]_2$.

$Ir_2(\mu\text{-DArF})_4(\eta^1\text{-}O_2CCF_3)\cdot 2CH_2Cl_2$. The compound with Ar = *p*-anisyl crystallized in the orthorhombic space group *Pbcn*,

---

(17) See for examples: (a) Cotton, F. A.; Murillo, C. A.; Stiriba, S.-E. *Inorg. Chem. Commun.* **1999**, 463−464. (b) Appleton, T. G. *J. Chem. Educ.* **1977**, *54*, 443−444.

Table 3. Metal−Metal Distances (Å) for Some Paddlewheel-Type Group 9 Amidinate Species with M_2^{n+} Cores

			DArF,[b] ArN−X−NAr		
compound[a]	*n*	M−M distance (Å)	Ar	X	ref
$Co_2(\mu\text{-DPhF})_4$	4	2.3735(9)	phenyl	CH	18
$Co_2(\mu\text{-DPhBz})_4$	4	2.302(1)	phenyl	CPh	19
$Co_2(\mu\text{-DTolTA})_4$	4	2.265(2)	*p*-tolyl	N	10
$Co_2(\mu\text{-DPhBz})_4^+$	5	2.322(2) 2.332(2)	phenyl	CPh	18
$Rh_2(\mu\text{-DPhF})_4$	4	2.457(1)	phenyl	CH	20
$Rh_2(\mu\text{-DPhF})_4(CH_3CN)$	4	2.459(1)	phenyl	CH	20
$Rh_2(\mu\text{-DPhBz})_4$	4	2.389(1)	phenyl	CPh	19
$Rh_2(\mu\text{-DTolF})_4$	4	2.4336(4)	*p*-tolyl	CH	21
$Rh_2(\mu\text{-DAni}^m\text{F})_4$	4	2.452(1) 2.415(1)	*m*-anisyl	CH	22
$Rh_2(\mu\text{-DPh}^{Cl_2}\text{F})_4$	4	2.458(1)	3,5-dichlorophenyl	CH	22
$Rh_2(\mu\text{-DTolF})_4[(\eta^1\text{-C(CN)}_3]$	5	2.463(4)	*p*-tolyl	CH	23
$[Rh_2(\mu\text{-DTolF})_4(H_2O)]^+$	5	2.452(2)	*p*-tolyl	CH	24
$[Rh_2(\mu\text{-DPhF})_4(CH_3CN)]^+$	5	2.466(1)	phenyl	CH	20
$Rh_2(\mu\text{-DTolF})_3(\eta^2\text{-NO}_3)_2$[c]	5	2.485(1)	*p*-tolyl	CH	25
cis,cis-$[Rh_2(\mu\text{-DTolF})_2(\mu\text{-O}_2CCF_3)_2(\eta^1,\eta^1\text{-O}_2CCF_3)Ag]_2$	5	2.448(2)	*p*-tolyl	CH	26
$Ir_2(\mu\text{-DTolF})_4$	4	2.524(3)	*p*-tolyl	CH	5
$Ir_2(\mu\text{-DAniF})_4(\eta^1\text{-O}_2CCF_3)$	5	2.5073(9)	*p*-anisyl	CH	this work
$Ir_2(\mu\text{-DPh}^{Cl}\text{F})_4(\eta^1\text{-O}_2CCF_3)$	5	2.513(1)	*p*-chlorophenyl	CH	this work
$Ir_2(hpp)_4Cl_2$[d]	6	2.495(1)			6

[a] For the amidinate ligands, the following abbreviations have been used: F = formamidinate, Bz = benzamidinate, TA = triazenate; thus, DPhF represents the *N,N'*-diphenylformamidinate anion. [b] Ar = aryl group. [c] Strictly speaking, this is not a paddlewheel complex but is given here as a reference. [d] hpp is not an amidinate group, but it is related to them because it contains a mononegative N−C−N unit; it represents the anion of 1,3,4,6,7,8-hexahydro-*2H*-pyrimido[1,2-*a*]pyrimidine.

Scheme 1

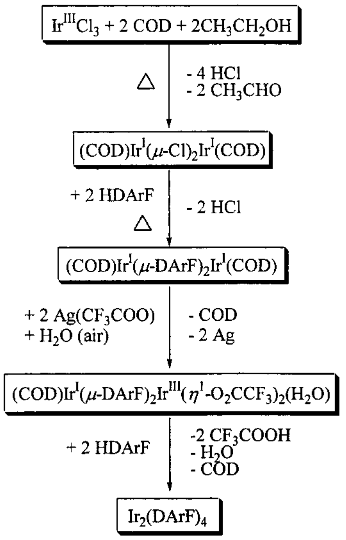

Scheme 2

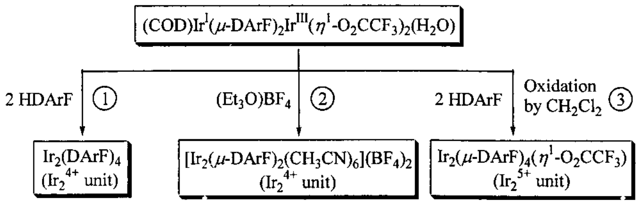

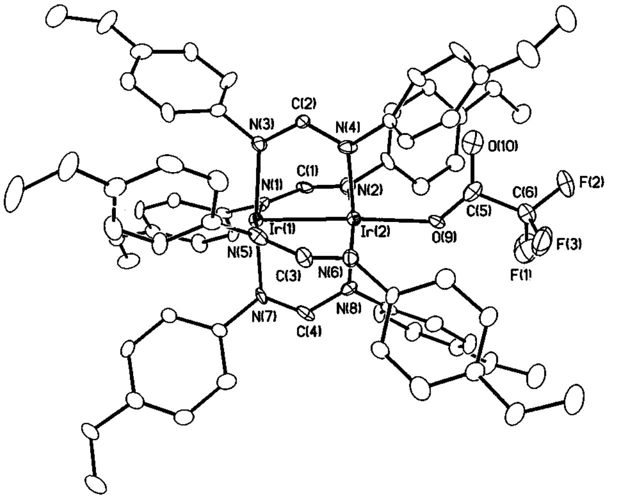

Figure 2. A drawing of the molecular structure of $Ir_2(\mu\text{-DAniF})_4(\eta^1\text{-O}_2CCF_3)$, with ellipsoids drawn at the 40% probability level.

and the *p*-chlorophenyl analogue in the monoclinic space group *P*2/*n*, but the cores of the two compounds are very similar. As shown in Figure 2 the Ir_2^{5+} unit is bridged by four formamidinate ligands. A carboxylate group is unsymmetrically bound to only one of the iridium atoms. The two metal atoms are separated by 2.5073(9) and 2.513(1) Å, and the average N−Ir−Ir−N torsion angles are 15.6° and 11.8° for the *p*-anisyl and *p*-chlorophenyl complexes, respectively. As listed in Table 3, the Ir−Ir bond distances of the Ir_2^{5+} cores are slightly shorter than that of the Ir_2^{4+} core, but longer than that of the Ir_2^{6+} core. This variation is consistent with the change from a single bond in the Ir_2^{4+} unit to a formal bond order of 1.5 in Ir_2^{5+} to a double

---

(18) Cotton, F. A.; Daniels, L. M.; Feng, X.; Maloney, D. J.; Matonic, J. H.; Murillo, C. A. *Inorg. Chim. Acta* **1997**, *256*, 291−301.

(19) He, L.-P.; Yao, C.-L.; Naris, M.; Lee, J. C.; Korp, J. D.; Bear, J. L. *Inorg. Chem.* **1992**, *31*, 620−625.

(20) Bear, J. L.; Yao, C.-L.; Lifsey, R. S.; Korp, J. D.; Kadish, K. M. *Inorg. Chem.* **1991**, *30*, 336−340.

(21) Piraino, P.; Bruno, G.; LoSchiavo, S.; Laschi, F.; Zanello, P. *Inorg. Chem.* **1987**, *26*, 2205−2211.

(22) Ren, T.; Lin, C.; Valente, E. J.; Zubkowski, J. D. *Inorg. Chim. Acta* **2000**, *297*, 283−290.

(23) LoSchiavo, S.; Bruno, G.; Zanello, P.; Laschi, F.; Piraino, P. *Inorg. Chem.* **1997**, *36*, 1004−1012.

(24) Bruno, G.; LoSchiavo, S.; Tresoldi, G.; Piraino, P.; Valli, L. *Inorg. Chim. Acta* **1992**, *196*, 131−136.

(25) Piraino, P.; Bruno, G.; Nicolò, F.; Faraone, F.; LoSchiavo, S. *Inorg. Chem.* **1985**, *24*, 4760−4762.

(26) Bruno, G.; Tresoldi, G.; LoSchiavo, S.; Sergi, S.; Piraino, P. *Inorg. Chim. Acta* **1992**, *197*, 9−14.

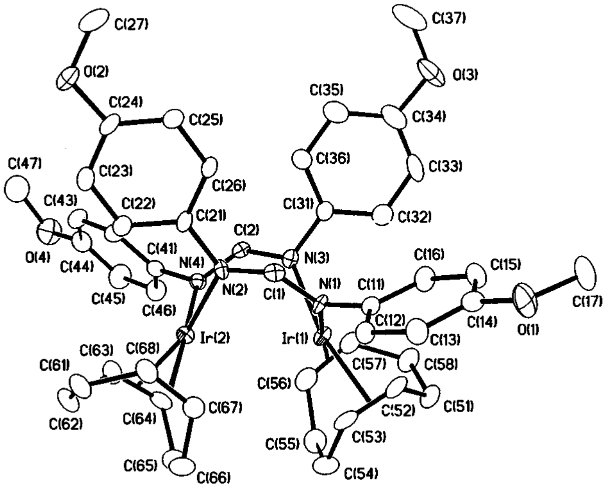

Figure 3. A plot of the $Ir_2(DAniF)_2(COD)_2$ molecule. Atoms are represented by their 40% probability ellipsoids.

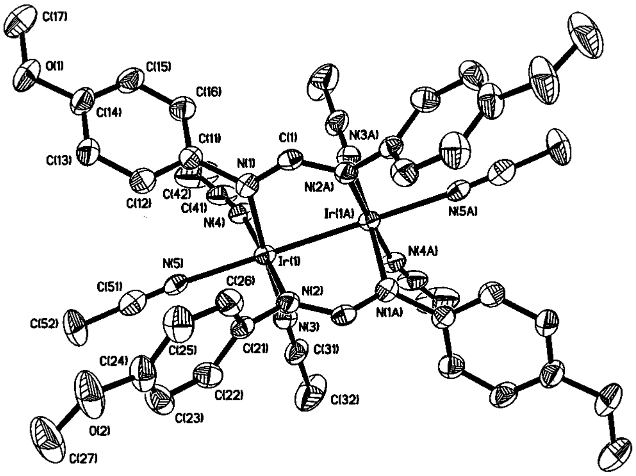

Figure 4. A drawing of the cation $[Ir_2(cis\text{-}\mu\text{-}DAniF)_2(CH_3CN)_6]^{2+}$, with ellipsoids drawn at the 40% probability level.

bond in Ir_2^{6+}. Unfortunately, it is hard to assess how meaningful these changes of less than 0.03 Å may be since there are not enough structurally characterized compounds to make comparisons, and one cannot rule out that this correlation might be fortuitous. It is known that variations in steric demand and electronic characteristics of the ligands can have important effects in some dimetal units. This is illustrated in Table 3, which lists the known paddlewheel-type group 9 amidinate species. For cobalt there is actually an increase in the Co−Co distance as the oxidation state of the metal atoms increases, while a clear trend is not easily seen for the rhodium complexes. Therefore, it is hard to tell the precise electronic configuration of these M_2^{n+} cores solely on the basis of their structures without other data and comprehensive theoretical calculations. The EPR spectrum of the *p*-anisyl derivative in frozen CH_2Cl_2 solution at −100 °C is consistent with the presence of an unpaired electron; it shows a ground state of $S = 1/2$ with a g_{iso} of 2.14, which is consistent with a $\sigma^2\pi^4\delta^2\delta^{*2}\pi^*$ configuration.

$[Ir(DAniF)(COD)]_2$·toluene. The X-ray structure of this dimetal compound is depicted in Figure 3. The compound crystallized in the monoclinic space group $P2_1/c$. Each Ir atom has square planar coordination with chelating COD molecules and bridging $DAniF^-$ ligands. An Ir···Ir distance of 3.2327(6) Å indicates that there is no bond between these two atoms. The average N−Ir−Ir−N torsion angle is 27.4°.

$[Ir_2(cis\text{-}\mu\text{-}DAniF)_2(MeCN)_6](BF_4)_2\cdot 2CH_3CN$. This compound crystallized in the monoclinic space group *P*2/*n*. The structure of this molecule, as shown in Figure 4, is very similar to that of its *p*-tolyl analogue. Two μ-formamidinate ligands are in a cis configuration, while two CH_3CN molecules are ligated in the axial positions. The Ir−Ir distance of 2.6019(4) Å is essentially the same as that of 2.601(1) Å in the *p*-tolyl analogue. The average N−Ir−Ir−N torsion angle is 18.7°.

Acknowledgment. We are grateful to the National Science Foundation for support and to Dr. Lee M. Daniels for helpful crystallographic advice.

Supporting Information Available: An X-ray crystallographic file, in CIF format. This material is available free of charge via the Internet at http://pubs.acs.org.

IC000527C